

Correlation Equation for Predicting Single-Collector Efficiency in Physicochemical Filtration in Saturated Porous Media

NATHALIE TUFENKJI AND
MENACHEM ELIMELECH*

Department of Chemical Engineering, Environmental
Engineering Program, P.O. Box 208286, Yale University,
New Haven, Connecticut 06520-8286

A new equation for predicting the single-collector contact efficiency (η_0) in physicochemical particle filtration in saturated porous media is presented. The correlation equation is developed assuming that the overall single-collector efficiency can be calculated as the sum of the contributions of the individual transport mechanisms—Brownian diffusion, interception, and gravitational sedimentation. To obtain the correlation equation, the dimensionless parameters governing particle deposition are regressed against the theoretical value of the single-collector efficiency over a broad range of parameter values. Rigorous numerical solution of the convective–diffusion equation with hydrodynamic interactions and universal van der Waals attractive forces fully incorporated provided the theoretical single-collector efficiencies. The resulting equation overcomes the limitations of current approaches and shows remarkable agreement with exact theoretical predictions of the single-collector efficiency over a wide range of conditions commonly encountered in natural and engineered aquatic systems. Furthermore, experimental data are in much closer agreement with predictions based on the new correlation equation compared to other available expressions.

Introduction

The transport and deposition (physicochemical filtration) behavior of colloidal particles in saturated porous media is of considerable interest in numerous processes in natural and engineered systems. A thorough understanding of particle filtration is essential for predicting the transport and fate of microbial particles, such as bacteria, viruses, and protozoan (oo)cysts as well as colloid-bound pollutants in subsurface environments (1–4). Particle transport and deposition are also the basis of deep-bed (granular) filtration, a unit operation commonly used in water and wastewater treatment and other industrial separations (5).

The transport of colloidal particles from the pore fluid to the vicinity of a filter grain (collector) is typically described by three mechanisms: interception, gravitational sedimentation, and Brownian diffusion. Transport of particles by interception occurs when a particle moving along a streamline comes into contact with the collector due to its finite size. Gravitational sedimentation refers to the settling of particles

with densities greater than that of the fluid onto the collector surface. Smaller particles undergo Brownian motion (diffusion), which can result in contact with the collector grains.

Yao et al. (5) presented the first water filtration model suggesting that the three transport mechanisms are additive. The classic filtration model of Yao et al. (5), however, does not consider the influence of hydrodynamic (viscous) interactions and the universal van der Waals attractive forces. Accurate predictions of colloid filtration (i.e., including hydrodynamic and van der Waals interactions) can be obtained by numerical solution of the convective–diffusion equation (6, 7) or trajectory analysis for non-Brownian particles (8). Results of such rigorous approaches reveal that hydrodynamic interactions play a very important role in the filtration behavior of colloidal particles, especially for particles larger than a few tenths of a micrometer (6, 7).

Since numerical solution of the convective–diffusion equation or trajectory analysis is not straightforward and is not readily available for use, a semiempirical approach for predicting filtration efficiency would be quite useful. Such a semiempirical correlation equation for the single-collector contact efficiency (usually denoted as η_0) in packed-bed (granular) filtration was developed by Rajagopalan and Tien (9) by solving numerically the trajectory equation for non-Brownian particles. The correlation equation of Rajagopalan and Tien (RT) has been used extensively to predict the deposition (filtration) of colloidal particles in natural and technological systems (10–13). However, the RT equation has several limitations (to be discussed later in the paper) that render the equation inaccurate for prediction of filtration efficiency for most conditions of practical relevance. The major shortcoming of the RT equation is the omission of the influence of hydrodynamic and van der Waals interactions on the deposition of particles that are dominated by Brownian diffusion. The latter removal mechanism may extend to particles as large as a few micrometers for filtration at low Peclet numbers or flow rates (such as in subsurface environments), thus covering the entire range of microbial particles of environmental relevance. Hence, a more accurate and complete expression for predicting the single-collector efficiency in filtration in saturated porous media is needed.

A new correlation equation for calculating the single-collector efficiency for physicochemical filtration in saturated porous media is presented in this paper. The equation is based on a rigorous numerical solution of the convective–diffusion equation with all particle-removal mechanisms and interaction forces considered. Predictions of single-collector efficiencies with the correlation equation over a wide range of parameter values show remarkable agreement with exact theoretical values based on numerical solution of the convective–diffusion equation. In addition, experimental data are in much closer agreement with predictions using the newly developed correlation equation compared to other available expressions.

Convective–Diffusion Equation for Rigorous Description of Filtration

Governing Equation and Boundary Conditions. The transport and deposition of colloidal particles in saturated homogeneous porous media is described by the convective–diffusion equation. Under steady-state conditions, the general form of the convective–diffusion equation is given by (6)

$$\nabla \cdot (\mathbf{u}C) = \nabla \cdot (\mathbf{D} \cdot \nabla C) - \nabla \cdot \left(\frac{\mathbf{D} \cdot \mathbf{F}}{kT} C \right) \quad (1)$$

* Corresponding author phone: (203)432-2789; fax: (203)432-2881; e-mail: menachem.elimelech@yale.edu.

TABLE 1. Summary of Dimensionless Parameters Governing Particle Filtration

parameter	definition ^a	physical interpretation
N_R	$\frac{d_p}{d_c}$	aspect ratio
N_{Pe}	$\frac{Ud_c}{D_\infty}$	Peclet number characterizing ratio of convective transport to diffusive transport
N_{vdW}	$\frac{A}{kT}$	van der Waals number characterizing ratio of van der Waals interaction energy to the particle's thermal energy
N_{gr}	$\frac{4}{3} \frac{\pi a_p^4 (\rho_p - \rho_f) g}{kT}$	gravitational number; ratio of particle's gravitational potential when located one particle radius from collector to particle's thermal energy
N_A	$\frac{A}{12\pi\mu a_p^2 U}$	attraction number; represents combined influence of van der Waals attraction forces and fluid velocity on particle deposition rate due to interception
N_G	$\frac{2}{9} \frac{a_p^2 (\rho_p - \rho_f) g}{\mu U}$	gravity number; ratio of Stokes particle settling velocity to approach velocity of the fluid

^a The parameters in the various dimensionless groups are as follows: d_p is the particle diameter, d_c is the collector diameter, U is the fluid approach velocity, D_∞ is the bulk diffusion coefficient (described by Stokes–Einstein equation), A is the Hamaker constant, k is the Boltzmann constant, T is fluid absolute temperature, a_p is particle radius, ρ_p is the particle density, ρ_f is the fluid density, μ is the absolute fluid viscosity, and g is the gravitational acceleration.

where C is the fluid-phase particle concentration, \mathbf{D} is the particle diffusion tensor, \mathbf{u} is the particle velocity vector induced by fluid flow, k is the Boltzmann constant, T is the absolute temperature, and \mathbf{F} is the external force vector. The terms on the right-hand side of eq 1 describe the transport of particles induced by diffusion and external forces, respectively, whereas the term on the left-hand side accounts for convective transport. The external forces of interest here are the attractive van der Waals force and gravity. Details on the formulation of the various terms in eq 1, the incorporation of hydrodynamic interactions, the inclusion of external (retarded van der Waals and gravitational) forces, and the nondimensionalization of the equation are provided elsewhere (14).

For convenience in numerical calculations, eq 1 can be rewritten as (14)

$$\frac{\partial C^*}{\partial \theta} = a_1(H, \theta) \frac{\partial^2 C^*}{\partial H^2} + a_2(H, \theta) \frac{\partial C^*}{\partial H} + a_3(H, \theta) C^* \quad (2)$$

Here, $C^*(H, \theta)$ is the dimensionless concentration distribution of particles around a spherical collector; H is the dimensionless surface-to-surface separation distance between a particle and the collector; θ is the tangential coordinate; and $a_1(H, \theta)$, $a_2(H, \theta)$, and $a_3(H, \theta)$ are variable coefficients that can be determined from a detailed derivation of eq 1.

For the filtration problem at hand, the following boundary conditions are used to solve eq 2 (7, 14):

$$C^*(H = 0, \theta) = 0 \quad (3a)$$

$$C^*(H \rightarrow \infty, \theta) = 1 \quad (3b)$$

$$\left(\frac{\partial C^*}{\partial \theta} \right)_{\theta=0} = 0 \quad (3c)$$

The first boundary condition states that all particles reaching the collector surface ($H = 0$) are removed from the dispersed phase (the well-known perfect-sink model). In the second boundary condition, the concentration of particles at a large distance from the collector surface is assumed to be equal to the bulk fluid concentration, C_0 . Since we use the Happel sphere-in-cell model (15) to describe the flow field in the porous medium, this boundary condition is taken at the outer surface of the Happel's fluid envelope, where its thickness (b) is given by $b = a_c(1 - f)^{-1/3}$ (a_c is the radius of the spherical

collector and f is the porosity of the porous medium). The third boundary condition arises from the symmetry around the forward stagnation path (7). It is important to note that the mechanism of interception is accounted for in the perfect-sink boundary condition (eq 3a) as the particle velocity is calculated at the center of the particle (5, 6). The two other transport mechanisms (gravitational sedimentation and Brownian diffusion) are included in the governing equation (eq 1) as described above.

Dimensionless Parameters Governing Particle Filtration. Upon nondimensionalization of eq 1, we note that the single-collector contact efficiency can be expressed as a function of four dimensionless groups (6, 7):

$$\eta_0 = \eta_0(N_R, N_{Pe}, N_{vdW}, N_{gr}) \quad (4)$$

where N_R is an aspect ratio, N_{Pe} is the Peclet number, N_{vdW} is the van der Waals number, and N_{gr} is the gravitational number. The definitions and physical interpretations of these dimensionless parameters (and two other parameters, N_A and N_G , to be defined later) are provided in Table 1.

Determination of Single-Collector Contact Efficiency. When the effects of van der Waals forces, gravity, and hydrodynamic interactions are considered simultaneously, there are no analytical solutions to the convective–diffusion equation. The problem described by eqs 2 and 3 can be solved numerically as described by Elimelech (14). Once the dimensionless concentration distribution of particles around the collector, $C^*(H, \theta)$, is determined, the perpendicular flux of particles at the collector surface can be calculated. The overall rate of particle collisions with the collector (I) is obtained by integration of the particle flux (at $H = 0$) over the entire surface of the spherical collector. Finally, the single-collector contact efficiency (η_0) is obtained as the ratio of the overall rate of particle deposition onto the collector (I) to the convective transport of upstream particles toward the projected area of the collector (5):

$$\eta_0 = \frac{I}{\pi a_c^2 U C_0} \quad (5)$$

where U is the approach velocity of the fluid.

Validation of Numerical Scheme with Limiting Analytical Solutions. Since there is no analytical solution to the problem described by eqs 2 and 3, the numerical approach applied

here must be validated with limiting analytical solutions obtained by making several simplifying assumptions.

For Brownian-sized particles and in the absence of external forces and hydrodynamic interactions, the convective–diffusion equation can be solved analytically (the so-called Smoluchowski–Levich approximation) (6, 16). Under these conditions, the single-collector contact efficiency for a porous medium when using Happel’s flow model is given by

$$\eta_0 = 4.04 A_S^{1/3} N_{Pe}^{-2/3} \quad (6)$$

Here, A_S is a porosity-dependent parameter defined as

$$A_S = \frac{2(1 - \gamma^5)}{2 - 3\gamma + 3\gamma^5 - 2\gamma^6} \quad (7)$$

where $\gamma = (1 - f)^{1/3}$. In the derivation of eq 6, it was also assumed that the interception effect (due to the finite size of the particles) does not play a role in particle deposition. Calculations for very small particles (where interception is negligible) over a wide range of fluid approach velocities showed that particle deposition rates calculated from eq 6 and from a numerical solution of the convective–diffusion equation (under the assumptions discussed above) differed by less than 2%.

Another limiting analytical solution used to validate the numerical code is the classic interception equation (6, 7, 17):

$$\eta_0 = \frac{3}{2} A_S N_R^2 \quad (8)$$

where the aspect ratio N_R was defined earlier in Table 1. This equation is valid when the effects of Brownian diffusion, hydrodynamic interactions, van der Waals attraction forces, and gravitational forces are neglected. Comparison of calculations under the conditions where the classic interception equation holds (i.e., large Peclet number and the assumptions outlined above) showed that η_0 values calculated numerically were within a few percent of the corresponding values calculated from eq 8.

Development of a Correlation Equation for Predicting Single-Collector Contact Efficiency

General Approach and Parameter Range. Prieve and Ruckenstein (7) demonstrated that particle deposition rates calculated by summing individual contributions from each transport mechanism were in close agreement with deposition rates obtained from a rigorous solution of the convective–diffusion equation when all mechanisms are considered simultaneously. Here, we draw on the additivity assumption to develop our correlation equation for the single-collector contact efficiency:

$$\eta_0 = \eta_D + \eta_I + \eta_G \quad (9)$$

where η_D is the transport by diffusion, η_I is the transport by interception, and η_G is the transport due to gravity. A separate correlation equation is first determined for each mechanism (i.e., η_D , η_I , and η_G). Then, the overall single-collector efficiency is obtained by summing the individual contributions of each mechanism.

Previous studies (7, 9) suggest the three transport mechanisms to be power functions of multiple dimensionless parameters (e.g., $\eta_I = a N_R^b N_{Pe}^c N_{vdW}^d$, where a – d are constants). The values of the constants a – d for each correlation equation are obtained by performing a multiple linear regression analysis between the relevant dimensionless parameters and the corresponding single-collector contact efficiency. Thus, by numerically calculating the single-

TABLE 2. Summary of Parameter Values Used in Numerical Calculations

parameter	range
particle diameter, d_p	0.01–10 μm
collector (grain) diameter, d_c	0.05–0.50 mm
fluid approach velocity, U	7×10^{-6} – 2×10^{-3} m/s
Hamaker constant, A	3×10^{-21} – 4×10^{-20} J
particle density, ρ_p	1.0–1.8 g/cm ³
fluid absolute temperature, T	298 K
porosity, f	0.36

collector contact efficiency associated with each transport mechanism over a wide range of parameter values, a rigorous regression analysis can be carried out. Table 2 summarizes the values of the parameters used in our numerical calculations. The selected values of the parameters correspond to a wide range of dimensionless parameters and are relevant to most applications in aquatic systems.

Development of Correlations for η_D , η_I , and η_G . Based on the additivity assumption originally presented by Yao et al. (5) and later verified by Prieve and Ruckenstein (7), the overall single-collector contact efficiency (η_0) can be determined by summing the contributions of each transport mechanism. The methodology for obtaining the correlation equations for each transport mechanism is described in this section.

(a) Correlation for η_D . The contribution of the diffusion transport mechanism to the overall particle deposition rate is determined by “turning off” the remaining two mechanisms (i.e., interception and gravity). In numerical solution of the convective–diffusion equation, the interception mechanism is disabled by making a slight modification to the expressions describing the radial and tangential particle velocity components (14). When the radial coordinate in these expressions is defined such that the size of the colloidal particle is ignored (i.e., the particle is defined to be point-sized), the contribution due to interception is not taken into account. The contribution of gravity to the overall particle deposition rate is “turned off” by setting the density of the colloidal particles equal to the density of the bulk fluid (i.e., $\rho_p = \rho_f$).

To account for the influence of van der Waals attraction forces and hydrodynamic interactions on the diffusion mechanism, the single-collector contact efficiency was calculated numerically over the entire range of N_R , N_{Pe} , and N_{vdW} values (using variable ranges in Table 2) with the interception and gravity mechanisms disabled. As noted previously, the correlation equation for η_D is a power function of the relevant dimensionless parameters: $\eta_D = a N_R^b N_{Pe}^c N_{vdW}^d$. The values of the constants a – d in the correlation equation for η_D are determined by regressing the logarithm of the three dimensionless parameters (N_R , N_{Pe} , and N_{vdW}) against the logarithm of the calculated single-collector contact efficiency, resulting in

$$\eta_D = 2.4 A_S^{1/3} N_R^{-0.081} N_{Pe}^{-0.715} N_{vdW}^{0.052} \quad (10)$$

The adjusted coefficient of determination, R^2_{adj} , which takes into account the number of terms in the model, has a value of 0.997. The p values obtained from the multiple linear regression analysis indicate that all three dimensionless parameters are statistically significant predictors of η_D within 99% confidence.

It is interesting to note that based on the correlation presented here (eq 10), $\eta_D \sim d_p^{-0.796}$ as compared to $\eta_D \sim d_p^{-0.666}$ of the classic Levich solution (eq 6). This difference in the dependence of η_D on particle size reflects the significant influence of hydrodynamic interactions on the particle deposition rate. It is well-known (6, 18) that as particle size

increases, the influence of hydrodynamic (viscous) interactions becomes more significant. This is reflected in the steeper slope of the log–log plot of η_D versus d_p (i.e., higher absolute value of the d_p exponent).

(b) Correlation for η_I . Due to the nature of the numerical technique used here to solve the convective–diffusion equation, the contribution of diffusion to the rate of particle deposition cannot simply be disabled. Hence, we draw on the additivity assumption to determine the contribution of the interception mechanism to the overall particle deposition rate. First, the overall single-collector contact efficiency is calculated numerically for the case where we neglect the influence of gravity (i.e., $\eta_0 = \eta_D + \eta_I$) over the entire range of N_R , N_{Pe} , and N_{vdW} values. The contribution due to interception (η_I) is then obtained by subtracting η_D (also calculated numerically using the same parameter values) from η_0 . The correlation equation for η_I is determined similarly as described in the previous subsection for diffusion (case a), yielding

$$\eta_I = 0.55 A_S N_R^{1.55} N_{Pe}^{-0.125} N_{vdW}^{0.125} \quad (11)$$

Here, the adjusted coefficient of determination (R^2_{adj}) has a value of 0.998. As in the case for η_D , the p values obtained from the multiple linear regression analysis indicate that all three dimensionless parameters are statistically significant predictors of the single-collector contact efficiency within 99% confidence.

Previous studies (7, 9, 18, 19) have shown that, under conditions where the effects of Brownian diffusion and gravity can be neglected, the single-collector efficiency becomes a function of two dimensionless parameters. Careful inspection of the coefficients in eq 11 reveals that η_I can indeed be written as a function of two dimensionless parameters, N_R and N_A :

$$\eta_I = 0.55 A_S N_R^{1.675} N_A^{0.125} \quad (12)$$

where

$$N_A = \frac{A}{12\pi\mu a_p^2 U} \quad (13)$$

The attraction number (N_A) represents the combined influence of van der Waals attraction forces and fluid velocity on particle deposition rate due to interception. Note that $N_A = N_{vdW} N_R^{-1} N_{Pe}^{-1}$.

(c) Correlation for η_G . The contribution of the gravitational transport mechanism to the overall particle deposition rate is determined in a way similar to η_I . First, the overall single-collector contact efficiency is calculated numerically (i.e., $\eta_0 = \eta_D + \eta_I + \eta_G$) over the entire range of N_R , N_{Pe} , N_{vdW} , and N_{gr} values. The contribution due to gravity (η_G) is then obtained by subtracting $\eta = \eta_D + \eta_I$ (also calculated numerically using the same parameter values) from η_0 . The correlation equation for η_G is then determined by regressing the logarithm of the four dimensionless parameters (N_R , N_{Pe} , N_{vdW} , and N_{gr}) against the logarithm of the calculated single-collector efficiency (η_G) to yield:

$$\eta_G = 0.475 N_R^{-1.35} N_{Pe}^{-1.11} N_{vdW}^{0.053} N_{gr}^{1.11} \quad (14)$$

Here, the adjusted coefficient of determination (R^2_{adj}) has a value of 0.998. Once again, the p values obtained from the multiple linear regression analysis indicate that all four dimensionless parameters are statistically significant predictors of the single-collector contact efficiency within 99% confidence.

Careful inspection of the coefficients in eq 14 reveals that η_G can be written as a function of three dimensionless

parameters, N_R , N_{vdW} , and N_G :

$$\eta_G = 0.22 N_R^{-0.24} N_G^{1.11} N_{vdW}^{0.053} \quad (15)$$

where

$$N_G = \frac{2}{9} \frac{a_p^2 (\rho_p - \rho_f) g}{\mu U} \quad (16)$$

The new gravity number (N_G) represents the ratio of the Stokes particle settling velocity to the approach velocity of the fluid and, thus, better describes particle removal by gravitational sedimentation (5). Note that $N_G = 2 N_{gr} N_R^{-1} N_{Pe}^{-1}$.

Overall Correlation Equation for the Single-Collector Contact Efficiency. The overall single-collector contact efficiency for deposition in saturated porous media can now be written as the sum of the individual contributions for each transport mechanism (eqs 10, 12, and 15):

$$\eta_0 = 2.4 A_S^{1/3} N_R^{-0.081} N_{Pe}^{-0.715} N_{vdW}^{0.052} + 0.55 A_S N_R^{1.675} N_A^{0.125} + 0.22 N_R^{-0.24} N_G^{1.11} N_{vdW}^{0.053} \quad (17)$$

where the dimensionless parameters were previously defined in Table 1 and eq 7.

Representative results demonstrating the accuracy and versatility of the correlation equation under a broad range of parameter values relevant to processes in natural and engineered aquatic systems are shown in Figure 1. In Figure 1a, the single-collector contact efficiency (η_0) calculated from rigorous numerical solution of the convective–diffusion equation is compared to predictions based on the new correlation equation (eq 17) for conditions representative of colloidal or microbial transport in the subsurface environment (sandy aquifer), most notably low flow rate (10, 20). Similar comparisons for parameter values encountered in a riverbank filtration setting (21) and in deep-bed (granular) filtration in water treatment (22) are shown in Figure 1, panels b and c, respectively. These results demonstrate remarkable agreement between the new correlation equation and the exact (numerical) solution over the entire range of particle sizes. It is worthwhile to mention that, although the correlation equation was developed using the parameter values listed in Table 2, comparisons of calculations conducted beyond these ranges of values revealed very good agreement with rigorous numerical solution of the convective–diffusion equation. Similar successful comparisons for different values of the fluid (water) temperature (T) and bed porosity (f) further demonstrated the versatility of the new correlation equation.

Unique Features of the Correlation Equation. Inspection of the correlation equation (eq 17) reveals key differences when compared to current simplified approaches (5, 9) such as the commonly used RT equation (9). The difference most significant for environmental applications is observed in the first group of dimensionless parameters (i.e., η_D). In developing the correlation equation for the individual contribution of the diffusion mechanism, we considered the influence of hydrodynamic interactions and van der Waals forces. The effect of these important interactions is reflected in the dimensionless parameters N_R and N_{vdW} . However, in existing approaches, such as the RT equation, the influence of hydrodynamic interactions and van der Waals forces on transport by diffusion is not taken into account. Rather, the deposition of particles that are dominated by Brownian diffusion is described by the simplified Smoluchowski–Levich (16) approximation (eq 6) which consists only of the dimensionless parameter N_{Pe} .

Additional disparities between eq 17 and the RT equation are observed in the last group of dimensionless parameters

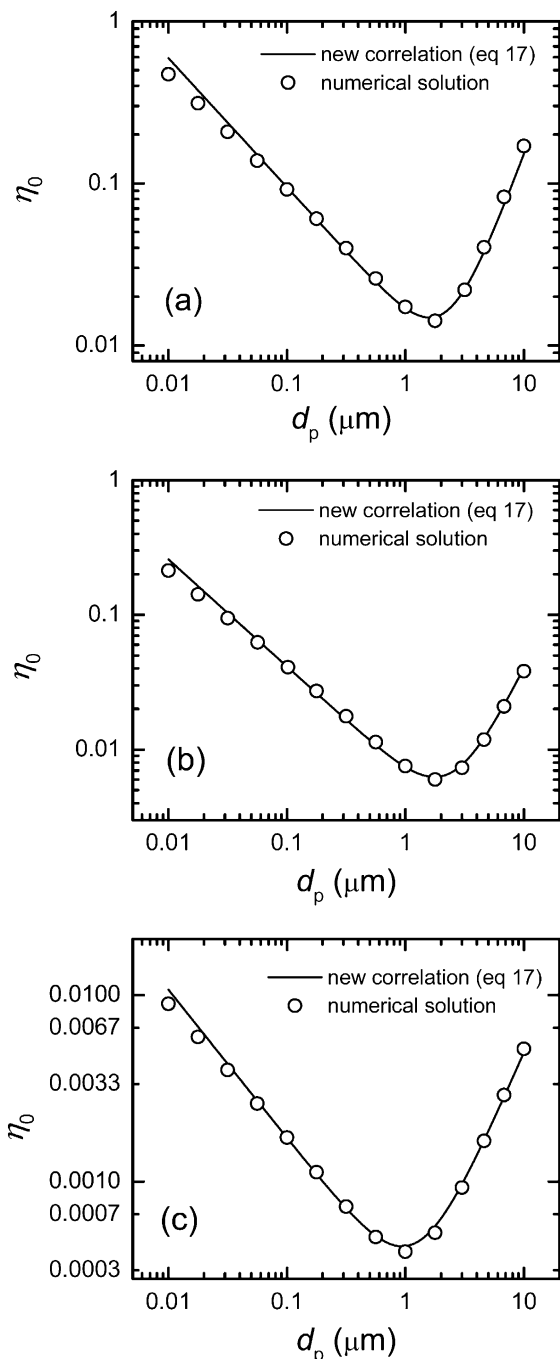


FIGURE 1. Comparison of predictions of single-collector contact efficiency (η_0) based on rigorous numerical solution of the convective–diffusion equation (open circles) and the new correlation equation, eq 17 (solid line), for three cases: (a) conditions typical of transport in sandy aquifers (10, 20): $d_c = 0.60$ mm, $U = 9 \times 10^{-6}$ m/s, $f = 0.39$, $A = 1 \times 10^{-20}$ J, $\rho_p = 1.05$ g/cm³, $T = 288$ K; (b) conditions encountered in riverbank filtration (27): $d_c = 0.40$ mm, $U = 4 \times 10^{-5}$ m/s, $f = 0.40$, $A = 1 \times 10^{-20}$ J, $\rho_p = 1.05$ g/cm³, $T = 288$ K; and (c) conditions typical of engineered (water treatment) systems (22): $d_c = 0.60$ mm, $U = 2.8 \times 10^{-3}$ m/s, $f = 0.40$, $A = 1 \times 10^{-20}$ J, $\rho_p = 1.05$ g/cm³, $T = 293$ K.

(i.e., η_G). First, we note that the porosity-dependent parameter A_S is not included in our correlation equation for η_G (eq 15), whereas it is present in the RT equation. Our calculations based on rigorous numerical solution of the convective–diffusion equation for different porosity values (i.e., $0.30 < f < 0.50$) revealed that η_G barely changes with porosity. Thus, the porosity-dependent parameter (A_S) should not be included in the contribution of the gravitational transport

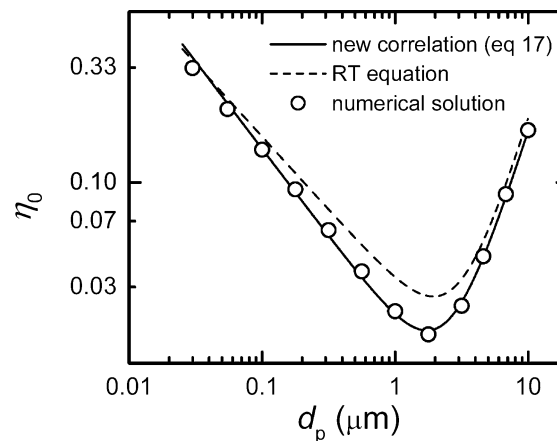


FIGURE 2. Comparison of predictions of single-collector contact efficiency (η_0) based on rigorous numerical solution of the convective–diffusion equation (open circles), the RT equation (dashed line), and the new correlation equation, eq 17 (solid line), for conditions where deposition is dominated by Brownian diffusion: $d_c = 0.40$ mm, $U = 8 \times 10^{-6}$ m/s, $f = 0.36$, $A = 1 \times 10^{-20}$ J, $\rho_p = 1.05$ g/cm³, $T = 288$ K.

mechanism. The other significant difference in η_G is the presence of the van der Waals number (N_{vdw}) in our correlation, whereas it is absent in other models (5, 9). Inherently, the universal van der Waals attraction force should be included in all three transport mechanisms. In fact, as mentioned previously, the linear regression analyses indicate that the van der Waals number is a significant predictor of the single-collector efficiency for each transport mechanism.

Comparison of New Correlation to RT Equation and Experimental Data

Comparison with the RT Correlation Equation. The RT equation has been used extensively to predict particle and microbial filtration in natural and technological systems. However, the RT equation has several limitations that render the equation inaccurate for prediction of single-collector contact efficiency under many conditions of practical relevance. In this section, we discuss the major shortcomings of the RT equation and compare predictions of η_0 with calculations based on our new correlation equation (eq 17).

The most important limitation of the RT equation is the exclusion of the influence of hydrodynamic interactions and van der Waals forces on the deposition of particles that are dominated by Brownian diffusion. Removal by the diffusion mechanism may be important for particles as large as a few micrometers for filtration at low flow rates (or low Peclet numbers), such as in groundwater aquifers. In Figure 2, the single-collector contact efficiency (η_0) calculated by rigorous numerical solution of the convective–diffusion equation is compared to predictions based on the RT equation as well as our new correlation equation (eq 17), for conditions where Brownian diffusion is important. The results clearly show how the RT equation significantly overestimates η_0 over a wide range of particle sizes in the Brownian regime (i.e., low N_{Pe}). For example, in the region where the single-collector efficiency reaches a minimum (i.e., $d_p \approx 2$ μ m), the calculations based on the RT equation are approximately 50% greater than the results of the numerical solution. The good agreement between the new correlation equation (eq 17) and the numerical solution demonstrates again the goodness of fit of the equation and underlines the importance of including van der Waals attraction forces and hydrodynamic interactions in these calculations.

The RT equation is often used to predict the filtration of microbial particles such as bacteria and protozoa in saturated

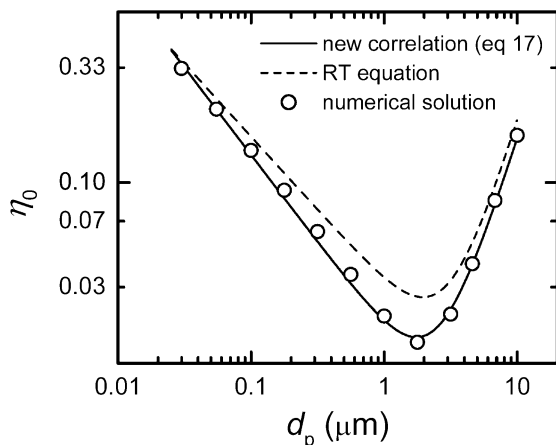


FIGURE 3. Comparison of predictions of single-collector contact efficiency (η_0) based on rigorous numerical solution of the convective-diffusion equation (open circles), the RT equation (dashed line), and the new correlation equation, eq 17 (solid line), for conditions where the deposition of microbial particles is dominated by Brownian diffusion: $d_c = 0.40$ mm, $U = 8 \times 10^{-6}$ m/s, $f = 0.36$, $A = 3 \times 10^{-21}$ J, $\rho_p = 1.05$ g/cm³, $T = 288$ K.

porous media (11–13). However, compared to most inorganic colloids (e.g., mineral colloids), microbial particles experience a lower van der Waals attraction force to mineral surfaces, such as quartz, due to relatively low Hamaker constants. For instance, in aqueous media, the Hamaker constant for a polio virus interacting with quartz is $3\text{--}5 \times 10^{-21}$ J (23), whereas for an inorganic silica colloid interacting with quartz, the Hamaker constant is much larger (1×10^{-20} J) (24). Thus, it is expected that the influence of hydrodynamic interactions will be more important in the deposition of microorganisms compared to other inorganic colloidal particles, since the lower attractive van der Waals force will not effectively counterbalance the retarding effect of hydrodynamic interactions.

In Figure 3, calculations of η_0 using rigorous numerical solution of the convective-diffusion equation are compared to predictions based on the RT equation as well as our new correlation equation (eq 17), for the same conditions used in Figure 2, with the exception that a lower Hamaker constant is used (i.e., $A = 3 \times 10^{-21}$ J). The results indicate an increased deviation between the predictions of the RT equation and the numerical solution of the convective-diffusion equation in comparison to the calculations shown in Figure 2, where a larger Hamaker constant ($A = 1 \times 10^{-20}$ J) was used. For a particle size of about $2 \mu\text{m}$, the RT predictions are now 60% greater than the η_0 values calculated numerically (as compared to 50% difference when $A = 1 \times 10^{-20}$ J).

Comparison with Experimental Data. In this section, the predictions of the new correlation equation; the RT equation (9); and the Yao, Habibian, and O'Melia (YHO) equation (5) are compared to data obtained from well-controlled laboratory-scale column experiments under chemical conditions where electrostatic double layer interactions were negligible (i.e., the attachment efficiency (α) approached unity). We have focused on experimental data where d_p ranges from approximately 0.1 to $4 \mu\text{m}$ since this is the range of particle diameters for which current simplified approaches (5, 9) warrant improvement. The data of Elimelech and O'Melia (25), Elimelech (26–28), Fitzpatrick (29), and Liu et al. (30) were chosen for this comparison because they were obtained from experiments using uniform, spherical latex particles and glass bead collectors. In addition, the experimental conditions under which these data were obtained cover a wide range of parameter values (particle size, approach velocity, and collector diameter) and are clearly

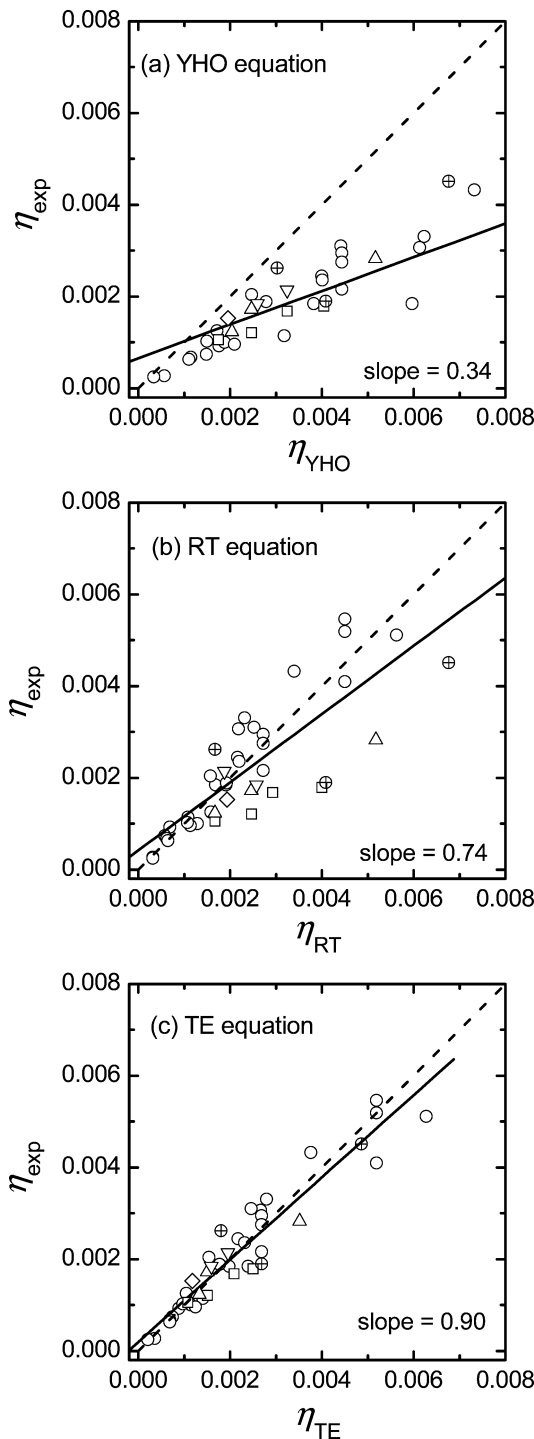


FIGURE 4. Comparison of experimental data with predictions of single-collector contact efficiency (η_0) based on (a) the YHO model, (b) the RT equation, and (c) the new TE correlation equation (eq 17). The dashed lines represent perfect agreement between experimental data and predictions, whereas the solid lines are the results of the linear regression analysis for each case. Experimental data taken from the following sources: (\circ) ref 29, (\square) ref 25, (\triangle) ref 26, (\oplus) ref 28, (\diamond) ref 27, and (∇) ref 30.

defined in each reference. The latex particles used have a density (ρ_p) ranging from 0.92 to 1.06 g/cm³, and the Hamaker constant (A) for the interaction of the latex particles with the glass bead collectors was reported to be 1×10^{-20} J.

In Figure 4a–c, the experimental data discussed above are plotted against the corresponding values of η_0 based on the YHO equation, the RT equation, and the present (TE)

equation (eq 17), respectively. In such plots, a slope of 1.00 and an intercept of zero are indicative of perfect agreement between experimental data and model predictions. In Figure 4a, the experimental data are compared to predictions of η_0 based on the YHO model with the inclusion of the porosity-dependent parameter (A_S) (5, 6). A linear regression of the data in Figure 4a (solid line) yields a slope of 0.34 and an intercept of 7×10^{-4} . In Figure 4b, the experimental data are plotted against the corresponding values of η_0 based on the RT equation. Here, a linear regression analysis yields a slope of 0.74 and an intercept of 4×10^{-4} . These results demonstrate how the RT equation improves upon the YHO model (i.e., slope closer to 1.00) by taking into account the influence of hydrodynamic interactions and van der Waals forces for the mechanisms of interception and gravitational sedimentation. In Figure 4c, the experimental data are compared to predictions of η_0 based on the new correlation equation (eq 17). In this case, a linear regression analysis yields a slope of 0.90 and an intercept of 2×10^{-4} .

The results of the linear regression analyses in Figure 4 clearly show that the predictions of η_0 based on the new correlation equation are in much better agreement with the experimental data than those based on the YHO and RT equations. More specifically, the deviation of the data from a slope of 1.00 and an intercept of zero (indicative of perfect agreement between experimental data and model predictions) is much smaller for the new correlation equation. In Figure 4a,b, the significantly smaller than unity (0.37 and 0.74, respectively) slopes indicate that the YHO and RT equations overestimate the experimental data, and this is in accord with our earlier discussion (Figures 2 and 3).

Applications of the New Correlation Equation. Under conditions relevant to most aquatic systems, the actual single-collector removal efficiency (η) is lower than the single-collector contact efficiency (η_0) due to repulsive colloidal interactions between particles and collector grains (6). The actual single-collector removal efficiency is often expressed as a product of an empirical attachment (collision) efficiency (α) and the single-collector contact efficiency:

$$\eta = \alpha \eta_0 \quad (18)$$

The attachment efficiency represents the fraction of collisions (contacts) between suspended particles and collector grains that result in attachment. Since current theories are inadequate to predict the attachment efficiency (4, 6, 25), it is common to use column experiments to determine the attachment efficiency for given physicochemical conditions (i.e., suspended particles, porous medium, and solution chemistry):

$$\alpha = -\frac{2}{3} \frac{d_c}{(1-f)L\eta_0} \ln(C/C_0) \quad (19)$$

Here, L is the filter medium packed length and C/C_0 is the column outlet normalized particle concentration at the initial stage of the particle breakthrough curve (5, 6). Equation 19 describes the ratio between the experimental single-collector removal efficiency (η) and the predicted single-collector contact efficiency (η_0) determined from eq 17.

When studying colloidal and microbial transport in saturated porous medium within the framework of the advection-dispersion equation (4), the rate of physicochemical filtration is often represented by the particle

deposition rate coefficient, k_d . The latter is related to the single-collector contact efficiency (η_0) by (2, 4)

$$k_d = \frac{3}{2} \frac{(1-f)}{d_c f} U \alpha \eta_0 \quad (20)$$

Note that the ratio of the approach (Darcy) velocity to the porosity in this equation (U/f) is the interstitial fluid velocity commonly used in particle transport modeling.

In deep-bed filtration, a key process in water and wastewater treatment, the filter coefficient (λ) is often used to express the removal of particles in the filter bed (6, 8, 17). The filter coefficient is related to the single-collector contact efficiency (η_0) via (6, 8)

$$\lambda = \frac{3}{2} \frac{(1-f)}{d_c} \alpha \eta_0 \quad (21)$$

Since chemical coagulants are used to destabilize particles in deep-bed filtration, the attachment efficiency $\alpha \approx 1$ (17). Thus, the single-collector contact efficiency (η_0) determined from eq 17 can be used to evaluate the particle removal efficiency in this type of process.

Acknowledgments

The authors acknowledge the support of the U.S. EPA (Award R-82901001-0) and the Natural Sciences and Engineering Research Council of Canada (NSERC) for a graduate student fellowship to N.T.

Nomenclature

Symbols

A	Hamaker constant
A_S	porosity-dependent parameter of Happel's model; $A_S = 2(1 - \gamma^5)/(2 - 3\gamma + 3\gamma^5 - 2\gamma^6)$
a_1, a_2, a_3	variable coefficients used in eq 2
a_c	radius of spherical collector
a_p	radius of particle
b	radius of the fluid envelope in Happel's model; $b = a_c(1 - f)^{-1/3}$
C	particle concentration
C_0	bulk (influent) particle concentration
C^*	dimensionless particle concentration, $C^* = C/C_0$
D	particle diffusion tensor
D_∞	diffusion coefficient in an infinite medium, $D_\infty = kT/(6\pi\mu a_p)$
d_c	diameter of spherical collector; $d_c = 2a_c$
d_p	diameter of particle; $d_p = 2a_p$
F	external force vector
f	porosity of a porous medium
g	gravitational acceleration, 9.81 m/s ²
H	dimensionless surface-to-surface separation distance (scaled with the particle radius)
I	overall particle deposition rate on a spherical collector
k	Boltzmann constant, 1.3805×10^{-23} J/K
k_d	particle deposition rate coefficient

L	filter medium packed length
N_A	attraction number; $N_A = A/(12\pi\mu a_p^2 U)$; note that $N_A = N_{vdW}N_R^{-1}N_{Pe}^{-1}$
N_G	gravity number obtained by combining three dimensionless parameters; $N_G = 2a_p^2(\rho_p - \rho_f) \times g/(9\mu U)$; note that $N_G = 2N_{gr}N_R^{-1}N_{Pe}^{-1}$
N_{gr}	gravitational force number; $N_{gr} = 4\pi a_p^4(\rho_p - \rho_f) \times g/(3kT)$
N_{Pe}	Peclet number; $N_{Pe} = Ud_c/D_\infty$
N_R	aspect ratio; $N_R = d_p/d_c$
N_{vdW}	van der Waals number; $N_{vdW} = A/kT$
R^2_{adj}	adjusted coefficient of determination
T	absolute temperature
t	time
U	approach (superficial) velocity of fluid
\mathbf{u}	particle velocity vector

Greek Letters

α	attachment efficiency
λ	filter coefficient
η_0	overall single-collector contact efficiency
η_D	single-collector contact efficiency for transport by diffusion
η_G	single-collector contact efficiency for transport by gravity
η_I	single-collector contact efficiency for transport by interception
θ	tangential (angular) coordinate around a spherical collector
μ	absolute viscosity of fluid
ρ_f	density of fluid
ρ_p	density of particle

Literature Cited

- (1) Tufenkji, N.; Ryan, J. N.; Elimelech, M. *Environ. Sci. Technol.* **2002**, *36*, 422A–428A.
- (2) Harvey, R. W.; Garabedian, S. P. *Environ. Sci. Technol.* **1991**, *25*, 178–185.
- (3) McCarthy, J. F.; Zachara, J. M. *Environ. Sci. Technol.* **1989**, *23*, 496–502.
- (4) Ryan, J. N.; Elimelech, M. *Colloid Surf. A* **1996**, *107*, 1–56.
- (5) Yao, K. M.; Habibian, M. T.; O'Melia, C. R. *Environ. Sci. Technol.* **1971**, *5*, 1105–1112.
- (6) Elimelech, M.; Gregory, J.; Jia, X.; Williams, R. A. *Particle Deposition and Aggregation: Measurement, Modelling, and Simulation*; Butterworth-Heinemann: Oxford, England, 1995.
- (7) Prieve, D. C.; Ruckenstein, E. *AIChE J.* **1974**, *20*, 1178–1187.
- (8) Tien, C. *Granular Filtration of Aerosols and Hydrosols*; Butterworth: Stoneham, MA, 1989.
- (9) Rajagopalan, R.; Tien, C. *AIChE J.* **1976**, *22*, 523–533.
- (10) Ryan, J. N.; Elimelech, M.; Baeseman, J. L.; Magelky, R. D. *Environ. Sci. Technol.* **2000**, *34*, 2000–2005.
- (11) Martin, R. E.; Bouwer, E. J.; Hanna, L. M. *Environ. Sci. Technol.* **1992**, *26*, 1053–1058.
- (12) Zhang, P. F.; Johnson, W. P.; Scheibe, T. D.; Choi, K. H.; Dobbs, F. C.; Mailloux, B. J. *Water Resour. Res.* **2001**, *37*, 2687–2698.
- (13) Hsu, B. M.; Huang, C. P.; Pan, J. R. *Water Res.* **2001**, *35*, 3777–3782.
- (14) Elimelech, M. *Sep. Technol.* **1994**, *4*, 186–212.
- (15) Happel, J. *AIChE J.* **1958**, *4*, 197–201.
- (16) Levich, V. G. *Physicochemical Hydrodynamics*; Prentice Hall: Englewood Cliffs, NJ, 1962.
- (17) Yao, K. M. Ph.D. Dissertation, University of North Carolina, 1968.
- (18) Spielman, L. A.; Fitzpatrick, J. A. *J. Colloid Interface Sci.* **1973**, *42*, 607–623.
- (19) Spielman, L. A.; Goren, S. L. *Environ. Sci. Technol.* **1970**, *4*, 135–140.
- (20) Ryan, J. N.; Elimelech, M.; Ard, R. A.; Harvey, R. W.; Johnson, P. R. *Environ. Sci. Technol.* **1999**, *33*, 63–73.
- (21) Schubert, J. In *Proceedings of the International Riverbank Filtration Conference*; Julich, W., Schubert, J., Eds.; IAWQ: Dusseldorf, Germany, 2000.
- (22) Cleasby, J. L. In *Water Quality and Treatment*, 4th ed.; Pontius, F. W., Ed.; McGraw-Hill: New York, 1990.
- (23) Murray, J. P. Ph.D. Dissertation. Stanford University, 1978.
- (24) Israelachvili, J. N. *Intermolecular and Surface Forces*, 2nd ed.; Academic Press: London, 1992.
- (25) Elimelech, M.; O'Melia, C. R. *Langmuir* **1990**, *6*, 1153–1163.
- (26) Elimelech, M. Ph.D. Dissertation, The Johns Hopkins University, 1989.
- (27) Elimelech, M. *J. Colloid Interface Sci.* **1991**, *146*, 337–352.
- (28) Elimelech, M. *J. Colloid Interface Sci.* **1994**, *164*, 190–199.
- (29) Fitzpatrick, J. A. Ph.D. Dissertation, Harvard University, 1972.
- (30) Liu, D. L.; Johnson, P. R.; Elimelech, M. *Environ. Sci. Technol.* **1995**, *29*, 2963–2973.

Received for review January 15, 2003. Revised manuscript received October 5, 2003. Accepted October 10, 2003.

ES034049R